energies

MDPI

Article

Life Evaluation of Battery Energy System for Frequency Regulation Using Wear Density Function

Jingyeong Park [1], Jeonghyeon Choi [1], Hyeondeok Jo [1], Daisuke Kodaira [2], Sekyung Han [1,3] and Moses Amoasi Acquah [4,*]

[1] School of Electronic and Electrical Engineering, Kyungpook National University, Daegu 41566, Korea
[2] Department of Electrical Engineering, Energy and Environment, University of Tsukuba, Tsukuba 305-8577, Ibaraki, Japan
[3] Department of Electrical Engineering, Kyungpook National University, Daegu 41566, Korea
[4] Department of Electrical Energy Engineering, Keimyung University, 1095 Dalgubeol-daero, Dalseo-gu, Daegu 42601, Korea
* Correspondence: amoasiacquah@gmail.com; Tel.: +82-10-5537-5122

Abstract: Frequency regulation (FR) using a battery energy storage system (BESS) has been expanding because of the growth of renewable energy. This study introduces the wear density function, which considers battery degradation factors such as the rate of current, temperature, and depth of discharge (DOD) to provide a precise lifespan prediction. Furthermore, an equivalent system model is developed to evaluate the FR performance of the BESS for various operating parameters. Finally, a quantitative tradeoff relationship between performance and battery lifecycle is derived from the analysis using operational data of the actual BESS for FR.

Keywords: battery management system; battery wear; energy storage system; frequency regulation; state of health

check for updates

Citation: Park, J.; Choi, J.; Jo, H.; Kodaira, D.; Han, S.; Acquah, M.A. Life Evaluation of Battery Energy System for Frequency Regulation Using Wear Density Function. *Energies* **2022**, *15*, 8071. https://doi.org/10.3390/en15218071

Academic Editors: Theodoros Kalogiannis and Md Sazzad Hosen

Received: 19 August 2022
Accepted: 25 October 2022
Published: 30 October 2022

Publisher's Note: MDPI stays neutral with regard to jurisdictional claims in published maps and institutional affiliations.

Copyright: © 2022 by the authors. Licensee MDPI, Basel, Switzerland. This article is an open access article distributed under the terms and conditions of the Creative Commons Attribution (CC BY) license (https://creativecommons.org/licenses/by/4.0/).

1. Introduction

Recent concerns about reducing greenhouse emissions have led to the mass introduction of renewable energy storage (RES) for ancillary grid services. These ancillary services have evolved to use battery energy storage systems (BESS) in their operation due to their inherent advantages. Compared with other traditional storage systems, BESS are modular, tractable, and have a fast and high-power density; this makes them suitable for many applications [1,2].

Recently there has been a shift from supply-oriented to demand-oriented policies as far as ESS is concerned. Korea Electric Power Corporation (KEPCO) had planned to invest $575 million to build a 500-MW battery BESS for frequency regulation (FR) [3]. Accordingly, KEPCO has constructed a total of 376-MW BESS since 2015. KEPCO owns and operates nine BESS substations, currently the largest in the world. Because of this, research on BESSs for FR has been rising, emphasising economic feasibility [4] and control methods [5]. Since KEPCO has been operating BESSs for years, they are focused on expanding the BESS operation algorithm based on assessing the lifecycle. It can be inferred that a tradeoff exists between the FR performance and battery lifecycle; therefore, the battery life should be evaluated first. However, the operating lifespan is currently only referenced to the battery manufacturer's warranty life. Many BESSs estimate the state of health (SoH) using the ratio of the accumulated usage capacity to available capacity for the lifetime. However, this is a rule-of-thumb value because the degradation varies considerably depending on the cycling pattern, such as temperature, charge/discharge rate, and depth of discharge (DoD) [6–8].

The representative existing methods for SoH estimation are as follows: (1) the reference performance test calculates the charge amount during discharging after being fully

charged [9]. This method is simple, highly accurate, and widely applied to electric vehicles [10]. However, the battery must be separated and assessed using a precise cycler, and the measurement could affect the lifespan [11,12]. (2) The internal impedance estimation method uses an inverse relationship with the SoH [13,14].

However, SoH for the same rated battery group produced by the same manufacturer exhibits considerable variation in the initial impedance and conductance. These values are affected by temperature and activation (polarisation) degrees [15,16] aside from battery conditions such as degradation. Furthermore, an accurate estimation during runtime is challenging because other components, such as contact resistance, would be included in the measured value. (3) The method for counting the charge/discharge cycle is frequently used in practice. In this method, the total transferrable lifecycle energy at a manufacturer-specific cycle condition (DoD 80%/0.5C-rate/room temperature) is used to yield the ratio to the actual transacted energy of the battery [16]. This method is the most convenient and inexpensive. However, the exact cycle pattern is usually more diverse than the considered cycle pattern; therefore, the actual degradation degree could vary considerably from the estimated value. (4) Model-based methods have been extensively studied in [17–21]. To estimate the SoH-related parameters, a specific battery model, the Randle equivalent circuit or electrochemical models, is employed. Various parameter estimation methods, such as the Kalman filter or sliding mode observer, can identify the battery degradation-related properties. However, in many cases, the model itself is inaccurate, and identifying the model parameter is challenging in a runtime environment [22]. The authors in [23] propose a data-driven SoH estimation method. With this method, the impact of essential ageing-relative parameters, such as temperature, rate of current, and state-of-charge (SoC), is quantitatively assessed via a pre-experiment for a target cell. An ageing evaluation model called a wear density function (WDF) is established, which can later be used to evaluate the degree of ageing for any arbitrary cycle pattern.

This study proposes a WDF method and performs various lifecycle evaluations with actual 24-MW (6 MWh) BESS operated for FR via KEPCO resources in Korea. The assessment results are compared with the conventional current-accumulation SoH estimation method to reveal the cycle pattern's impact on battery degradation. Furthermore, the impact of the FR operation parameter is quantitatively assessed for FR performance and battery life expectancy using the simulation model. The contributions of this paper are as follows:

- A laboratory experiment is performed to obtain the WDF parameters using the same battery packs in the field. The WDF is constructed for varying parameters, such as rate of charge/discharge (C-rate) and DoD. Consequently, wear cost ($/MWh) is obtained for each SoC level.
- The WDF is compared with the standard runtime input/output (I/O) energy-based method. Based on the actual operation data in the field, WDF-based life evaluation provides a more realistic and longer lifespan than the I/O energy-based method.
- The WDF evaluated an operating battery in the field while distinguishing transient to steady-state operation. The simulation results disclose the battery degradation rate from the parameter change for FR, such as droop rate, dead-band range, and SoC recovery range. Consequently, the tradeoff is quantitatively evaluated between FR capability and battery degradation.

This paper is organised as follows: Section 2 describes the theoretical background preceding the life evaluation method using the WDF. Section 3 compares the lifecycle assessment using the actual operation data of the previously specified battery energy storage system (BESS). Section 4 presents the lifecycle evaluation for the FR's control parameters using a predeveloped simulator, followed by the conclusions in Section 5.

2. Life Cycle Evaluation Method: WDF

2.1. Base Case: I/O Energy-Based Lifecycle Evaluation

In this subsection, the lifecycle of BESS is evaluated using a typical rule-of-thumb method implemented in many battery management systems of the existing BESS. This method estimates the SoH based on the amount of transferred I/O energy through the system. One major drawback of the conventional SoH estimation algorithm is the challenge of estimating the expected degree of degradation considering the actual usage pattern of the battery. Overall, specific fixed-cycle patterns are repeatedly applied to evaluate the impact on degradation. Figure 1 illustrates the achievable cycle count (ACC) until a specific end-of-life (EoL) condition regarding the cycled DoD. For instance, the tested cell can be cycled up to 2500 times using the DoD 20% cycle, a V-pattern cycle between SoC 100% and 80%.

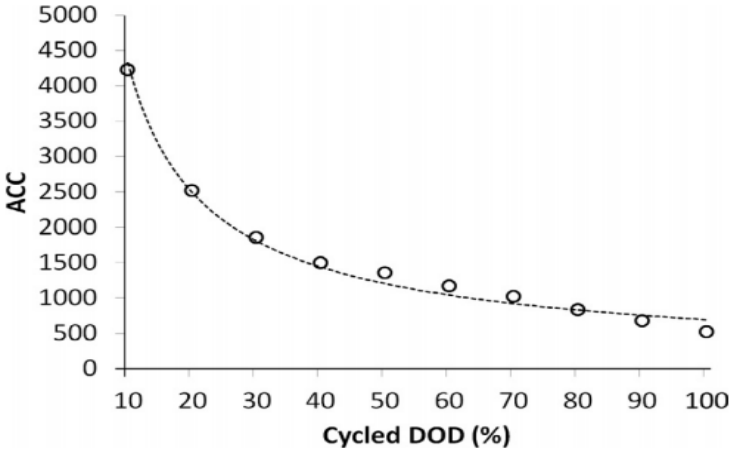


Figure 1. Lithium-ion DOD-ACC model.

It is challenging to provide sophisticated life predictions for complex usage patterns. DoD represents the V-pattern cycle, which repeatedly discharges from fully charged to SoC 80% and then charges to full. For example, Figure 1 shows the lifecycle data of a lithium-ion cell measured by increasing the DoD in units of 10%, showing only the change in the number of charge/discharge cycles. Because the actual usage pattern is usually not a V-pattern cycle, the DoD-ACC model is impractical in estimating the battery's degradation degree. The degradation amount occurring in the unit I/O energy must be determined for quantitative comparisons.

Therefore, in this study, the degradation according to DoD can be calculated using Equation (1) by introducing the concept of average wear cost (AWC) [21].

$$\begin{aligned} \mathrm{AWC(DoD)} &= \frac{Battery\ Price}{Total\ Transferrable\ Enerygy\ during\ the\ cycle} \\ &= \frac{Battery\ Price}{ACC(D) \times 2 \times DoD \times Battery\ Size \times Efficiency} \end{aligned} \tag{1}$$

For example, if the battery DoD is 40%, the ACC is 1500, the battery price is $10,000, the capacity is 16 kWh, and the charge/discharge efficiency is 0.9, Equation (1) produces $0.64/kWh; when the battery is repeatedly charged and discharged with a DoD of 40%, the wear cost is approximately $0.64/kWh. The degradation cost is the corresponding cost when the DoD is 40% charged and discharged. Therefore, the direct degradation cost cannot be estimated for a complex cycle pattern. In using a mobile phone, the degradation cost can be obtained if the battery is used only from 100% to 50% of the SoC and the battery is then fully charged again. However, the exact degradation cost is challenging to calculate because the actual (dynamic) charged/discharged use case needs to be defined.

Therefore, if the battery performs the charge/discharge with a DoD of 40%, the battery price can be evaluated as follows.

$$Battery\ Price = 2 \times ACC(0.4) \times \{AWC(0.4) \times DoD \times Battery\ Size\} \quad (2)$$

The AWC (0.4) in (2) is the AWC of DoD at 40%; thus, the SoC is repeatedly operated between 100% and 60%. If the degradation cost in each unit SoC interval can be obtained, rather than a fixed DoD interval, AWC can be expressed as the sum of the degradation costs. Therefore, the degradation cost function for a specific unit I/O energy is defined as W_d. The AWC is expressed as W_d, which can be expressed as (3):

$$Battery\ Price = 2 \times ACC(0.4) \times \{[W_d(0.6–0.7) + W_d(0.7–0.8) + W_d(0.8–0.9) + W_d(0.9–1)] \times 0.1 \times Battery\ size\}. \quad (3)$$

Assuming the SoC interval is divided by 10% in (3), W_d (0.6–0.7) means that the degradation cost occurred during the SoC operating range of 60–70%. Therefore, it can be expressed similarly as AWC (0.4) = W_d (0.6) + W_d (0.7) + W_d (0.8) + W_d (0.9). By further rearranging and solving this equation, we obtain:

$$\begin{aligned} AWC(0.4) &= W_d(0.6) + W_d(0.7) + W_d(0.8) + W_d(0.9) \\ &= \frac{Battery\ Price}{ACC(0.2) \times 2 \times 0.1 \times Battery\ Size \times \mu^2} \end{aligned} \quad (4)$$

where μ is the charging and discharging efficiency. Therefore, the degradation cost W of a specific unit section is defined as the degradation cost function W_d (s) for the unit I/O energy. If this is solved again using the normalised equation, (5) is obtained:

$$Battery\ Price = 2 \times ACC(D) \times \sum_{s=1-D}^{1-\Delta s} (W_d(s) \times \Delta q) \quad (5)$$

$\Delta q$is the amount of battery energy during the interval ΔS, and S is an instance in the SoC interval. When S is set to 10%, the DoD interval is 10, 20, 30, 100, and the total wear cost W_d per unit I/O for ten intervals can be expressed as (6).

$$\begin{aligned} W_d(0.9) &= \frac{Battery\ Price}{ACC(0.1) \times 2 \times 0.1 \times Battery\ Size \times \mu^2} \\ W_d(0.8) + W_d(0.9) &= \frac{Battery\ Price}{ACC(0.2) \times 2 \times 0.1 \times Battery\ Size \times \mu^2} \\ &\vdots \\ W_d(0) + \cdots + W_d(0.9) &= \frac{Battery\ Price}{ACC(1) \times 2 \times 0.1 \times Battery\ Size \times \mu^2} \end{aligned} \quad (6)$$

Because 10 unknowns $(W_d(0.1) \cdots W_d(0.9))$ and 10 cases of the DoD formula exist, the WDF can be obtained according to each SoC by:

$$\begin{bmatrix} 1 & 0 \cdots & \cdots 0 \\ 1 & 1\ 0 & \cdots 0 \\ \cdots & \cdots\cdots & \cdots\cdots \\ 1 & 1\ \ 1 & \cdots\ 1 \end{bmatrix} \begin{bmatrix} W_d(0.9) \\ W_d(0.8) \\ \cdots \\ W_d(0) \end{bmatrix} = \begin{bmatrix} \frac{Battery\ Price}{ACC\ (0.1) \times 2 \times 0.1 \times Battery\ Size \times\ \mu^2} \\ \frac{Battery\ Price}{ACC\ (0.2) \times 2 \times 0.1 \times Battery\ Size \times\ \mu^2} \\ \cdots \\ \frac{Battery\ Price}{ACC\ (1) \times 2 \times 0.1 \times Battery\ Size \times \mu^2} \end{bmatrix} \quad (7)$$

When the W_d(s) at each SoC point is multiplied by the energy I/O amount for the corresponding period, the degradation cost at the corresponding point can be obtained. Therefore, even if an arbitrary operation profile is provided, the degradation cost corresponding to the operation profile is derived by summing each point's degradation cost.

2.2. Operation Algorithm for BESS FR of KEPCO

The battery's operating pattern must be understood to evaluate the lifespan for FR because the stress on the battery depends on its FR control algorithm.

Therefore, we implemented the BESS control algorithm for FR, which is currently implemented in KEPCO (Figure 2). The system equivalent model simulator described in Figure 2 shows a flowchart of the implemented algorithm. The control algorithm of substation A operated by the 24-MW BESS for FR is divided into steady-state and transient-state control according to the frequency state [24]. When the system frequency deviates from the frequency dead-band (59.97 Hz–60.03 Hz), the governor-free operational mode by the droop is performed.

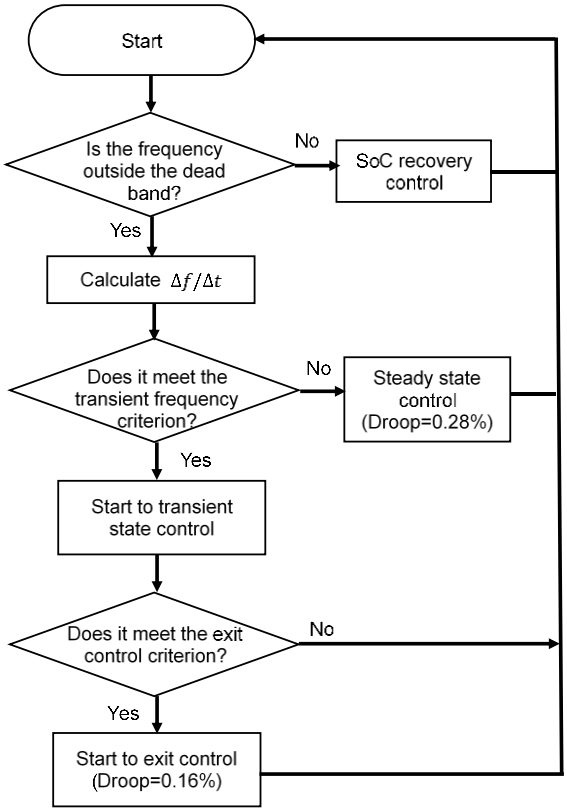


Figure 2. BESS's frequency regulation control algorithm [24].

At the beginning of the control, the BESS does not operate in the frequency dead-band to protect the facility by preventing frequent BESS operations. Thus, the energy in the battery is maintained when the frequency is stable. When this frequency dead-band is narrowed, frequent battery charges/discharges result in unnecessary battery damage in steady-state operations. If the frequency is within the dead-band, SoC recovery control is implemented. Recovery control is performed when SoC is less than 63% or more than 67%. The recovery control ends when SoC is between 64.5% and 65.5%. Therefore, if the recovery control's start condition changes, the number of operations and the C-rate change, changing the BESS's life. Transient control is performed by determining the target output of the system constant K (7870 MW/Hz) when the system frequency exceeds the frequency dead-band and meets the transient-state judgment criterion. The system constant K is an integer representing the relationship between the power system's power generation amount and the frequency variation because of the imbalance in the demand amount, and 1% of the maximum load is applied as a system constant. At the end of the transient state, if the system frequency is 59.9 Hz or higher and maintained for 1 s or longer, the droop performs the steady-state switching control and continues until the frequency is restored to 60 Hz. The droop is the rate of change in output regarding the frequency variation, and the droop controller is set to 0.28%, such that the BESS can supply power faster than the conventional generator. Because the droop defines the power system frequency characteristic as constant, K determines the BESS's charge and discharge target output. The constant K increases as

the speed adjustment ratio decreases, and the target output can be increased. Therefore, the battery's current rate is adjusted, affecting the BESS's life.

3. Life Cycle Evaluations in Current Operational Environment

This section evaluates the battery lifespan for a running BESS for FR in the field. Section 3.1 discusses the base case evaluation by I/O energy-based lifecycle evaluation deployed for the BESS. In Section 3.2, the proposed WDF evaluates the battery lifespan, which is more realistic considering other experimental field test projects.

3.1. Base Case: I/O Energy-Based Lifecycle Evaluation

In this subsection, the lifecycle of BESS is evaluated using a typical rule-of-thumb method implemented in many battery management systems of the existing BESS. This method estimates the SoH based on the amount of transferred I/O energy through the system. Therefore, we first analyse the total transferrable energy throughout the battery lifecycle at a specific cycle condition provided by the manufacturer. Second, the lifecycle regarding the usable years is calculated from the lifecycle energy and annual cycle energy ratio. We estimate the energy transferred for each BESS's operational mode to derive the expected annual energy.

With a sudden trip of the generator, the BESS's SoC decreases from 65% to 35% at a 4-C-rate. After it hits the bottom SoC, the algorithm tries recovering the SoC at a 0.2–0.4 charge rate (0.2-C–0.4-C-rate). The total duration, including the SoC recovering phase, lasts around an hour. Despite the harsh discharge, we confirmed that the cell temperature rises only by 5 °C because of air conditioning inside the container. This level is still insignificant (below 30 °C) for battery degradation. During the period, the total cycle energy is estimated to be around 3.45 MWh for the considered system. After analysing the annual report "System failure and frequency performance trend" issued by Korea Power Exchange (KPX) from 2012 to 2015, the authors confirmed that the transient condition happens, on average, four to five times yearly. From this result, the annual transient state I/O energy is calculated as approximately 17.25 MWh per year. The steady state operates when the grid frequency is maintained between 60 ± 0.028 Hz. Figure 3 shows the BESS's typical operating data during the steady state. The operating algorithm maintains the SoC at 65%. The temperature remains at 20 °C, and the C-rate is within 0.2-C. The average daily cycle (charge-discharge) energy in the steady state is estimated at 16.66 MWh from the operational data.

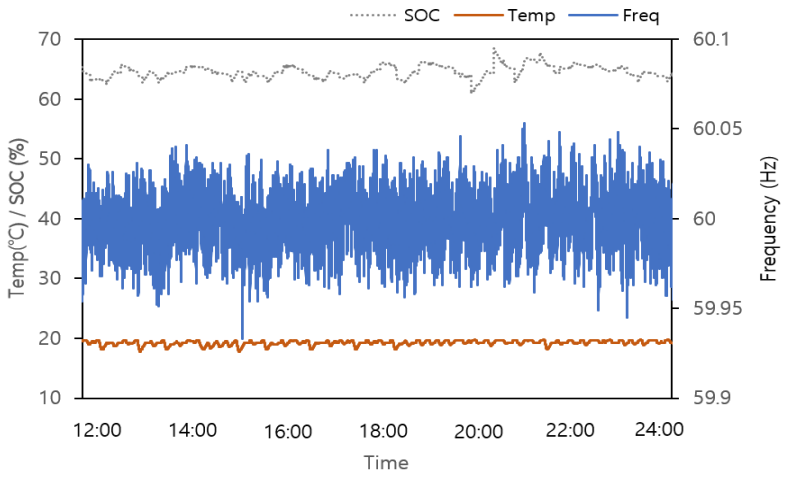


Figure 3. Actual steady-state operation of BESS on the grid.

Subsequently, the annual cycle energy caused during the steady state can be calculated as:

Annual cycle energy for steady state

$$\begin{aligned} &= E_{SS} \times \left(365 - \tfrac{n_{TS} \times T_{TS}}{24}\right) \\ &= 16.66\ \text{MWh} \times \left(365 - \tfrac{5 \times 1\ \text{h}}{24}\right) = 6076.7\ \text{MWh/year} \end{aligned} \tag{8}$$

where ESS (Energy Storage System) is the daily cycle energy for the steady state, n_{TS} is the number of annual transient states, and T_{TS} is the duration for each transient state (hourly). By combining the results from transient and steady states, the total annual I/O energy is given by:

Annual Total cycle energy

$$\begin{aligned} &= E_{TS} \times n_{TS} + E_{SS} \times \left(365 - \tfrac{n_{TS} \times T_{TS}}{24}\right) \\ &= 3.45\ \text{MWh} \times 5 \tfrac{\text{times}}{\text{year}} + \tfrac{6076.7\ \text{MWh}}{\text{year}} \\ &\cong 6094\ \text{MWh/year} \end{aligned} \tag{9}$$

where E_{TS} is the cycle energy during each transient state. Usually, including the one considered in this literature, BESSs supplied to the KEPCO should endure at least 4000 cycles at a DoD of 80% and a 0.5-C-rate. Therefore, the total I/O energy per 1 MWh of battery under the above lifecycle condition with 90% of cycle efficiency can be calculated as:

$$6\ \text{MWh} \times 0.8(DOD) \times 2(charge,\ discharge) \times 4000 Cycle \times 0.9^2 = 31,104\ \text{MWh} \tag{10}$$

Consequently, the expected lifespan of the BESS from the above method is estimated to be 31,104 MWh/6094 MWh/year = 5.1 years. Note that this is a conservative life expectancy, and it can be intuitively inferred that the actual battery life should be longer than the estimated value. An experimental field test of a BESS in California reports the degradation rate derived from a one-year operation [25]. Two cycles of charge and discharge occur daily. Consequently, the degradation rate is 7.7% for one year, which takes at least ten years to end a battery life. Complete charge and discharge cycles twice daily are harsher than the actual operation shown in Figures 3 and 4. The steady-state cycles of the battery are primarily in the middle SoC. It should result in far less degradation than the DoD cycle considered for life estimation, as the high and low SoC in the DoD cycle is usually more stressful than the middle SoC range. Therefore, this suggests the necessity for an elaborate assessment method considering degradation parameters.

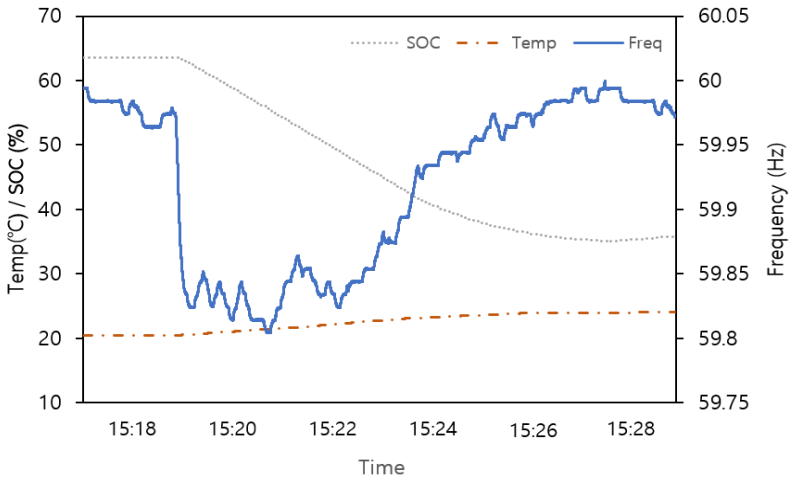


Figure 4. Typical operation profile for the FR BESS transient state.

3.2. Elaborated Assessment: Wear Density Funtion-Based Lifecycle Evaluation

Although the I/O energy-based method introduced in the previous section is often used in the field, its reliability is comparatively low because it does not consider the actual

operational environment affecting battery degradation. For example, the battery lifespan could vary considerably, depending on the trajectory of the SoC operation. To quantify the degradation factor, we evaluated the lifecycle using the WDF introduced in Section 2. The SoH estimation using the WDF quantifies the degradation stress depending on factors such as SoC, C-rate, and temperature. The stress is expressed as the wear cost per unit energy, and the I/O energy for each moment is multiplied by the weight derived from the WDF. Therefore, a more accurate result can be derived rather than only using the simple I/O-energy-based method because the weighting factor is included in the degradation factor. First, to derive the WDF, we conducted a lifecycle experiment assuming three operation scenarios: steady state, transient state, and manufacturer-specific 80% DoD cycle condition.

Figure 5 shows the battery cells being evaluated. The cell subjected to the lifecycle evaluation belongs to a major Korean cell manufacturer. The nominal capacity is 2850 mAh, the nominal voltage is 3.65 V, the discharge cut-off voltage is 2.5 V, and the cell type is 18650. The active cathode material is a lithium cell from the nickel-cobalt-aluminium series. The lifecycle test is conducted for 10–100% of the DoD at each 10% interval. In each cycle, the cells are fully charged under the constant current (CC)/constant voltage (CV) mode, and the cumulative discharge current and terminal voltages are logged during the discharge. The hybrid pulse power characterisation evaluates the capacity and power characteristics to measure the battery's capacity retention; this was evaluated at 135-Ah of the cumulative cycle energy.



Figure 5. Cells in a temperature chamber being cycled to derive WDF.

The test was conducted at a 0.5-C-rate and 25 °C until the capacity retention dropped to 91% for each cell. Figure 6 shows the trajectories as a solid line. Because the EoL condition is frequently defined as 80% of the capacity retention, the ACC for each cell is extrapolated to the EoL (dotted line). Figure 7 shows the resulting ACC versus DoD graph. The experiment is currently in progress and will continue varying the C-rate. In this study, the author's used pseudo-ACC-DoD data for 0.2-C and 4-C generated considering the results of preliminary experiments conducted by the authors. From the DoD-ACC graph, the WDF is derived from (6) regarding the C-rate, temperature, and SoC. During the calculation, the BESS's price is assumed to be $4.6 million for a unity 4C system (4 MW/1 MWh) based on the supply price announced by KEPCO [26]. Figure 8 shows the wear costs for each C-rate at 25 °C. From the figure, cycling at a high C-rate at both ends of the SoC wears the battery faster, which is typical.

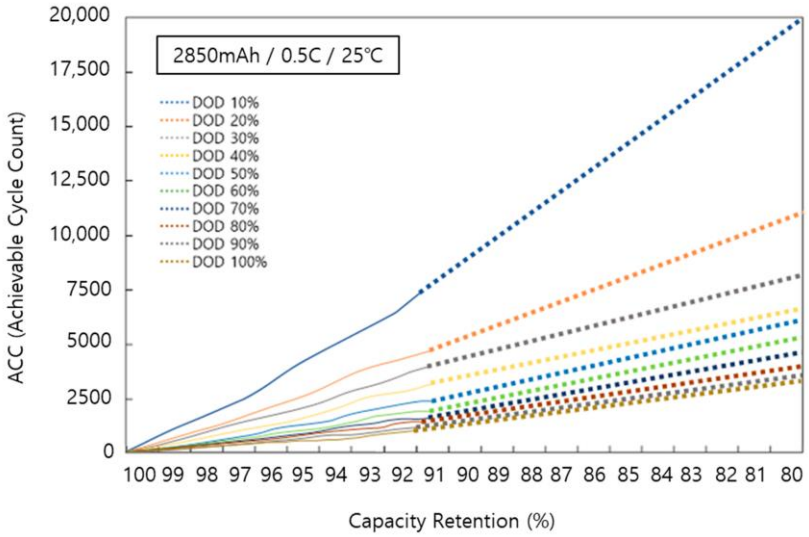


Figure 6. ACC life test by capacity retention.

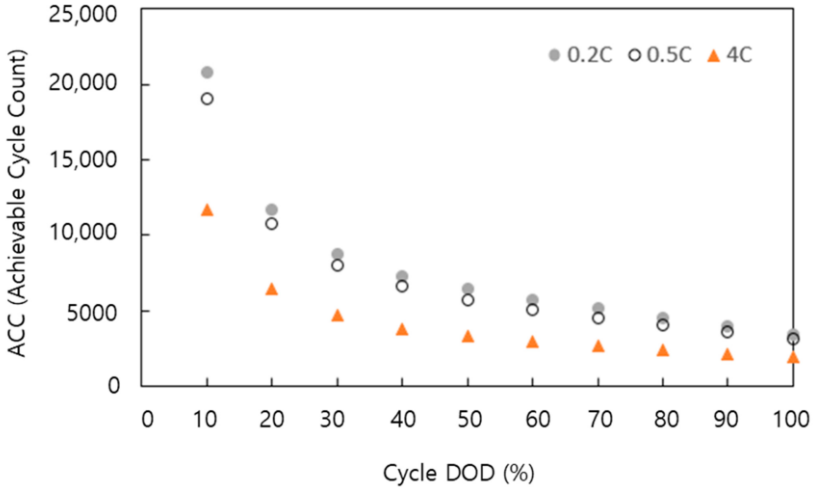


Figure 7. ACC vs. DOD at 25 °C.

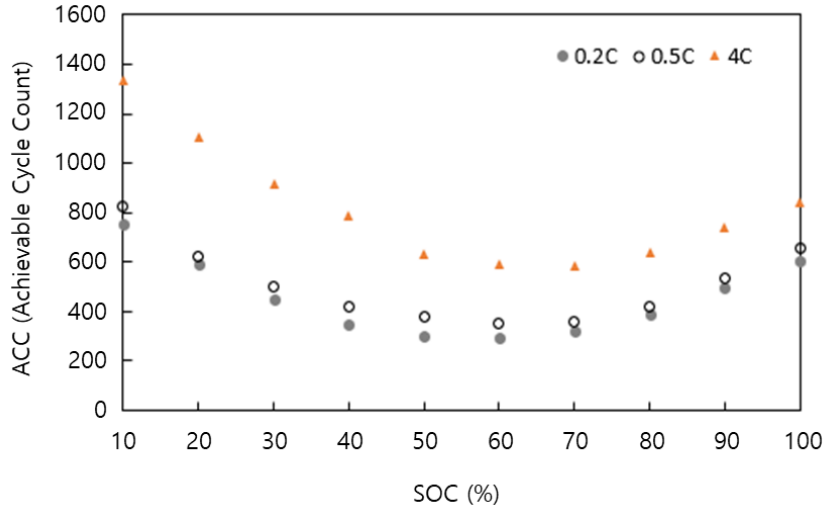


Figure 8. Wear cost for the BESS that costs $4.6 M per unity. A 4C system (4-MW/1-MWh) obtained using the DOD-ACC curve in Figure 4.

With the derived wear cost, the BESS's expected lifespan is evaluated for each operation mode, discussed in the previous section as:

$$Wear\ cost\ per\ mode = \sum_t \{W_d(s_t, T_t, c_t) \times q_t\} \tag{11}$$

where W_d is the WDF, s_t is the SoC, c_t is the C-rate, q_t is the amount of cycle energy for each time frame, and t is the time index during the given period.

The operating conditions for SoC, C-rate, and temperature are obtained for each time frame, and the corresponding wear cost is derived from the WDF (W_d). WDF values are obtained using linear interpolation between the adjacent points for conditions where the experiment is not conducted. The cycle energy is multiplied by the wear cost and integrated over the entire period. Table 1 shows the wear cost for each operation mode for the reference system being considered so far or 24-MW/6-MWh BESS with n_{TS} = 5.

Table 1. Wear cost calculated using WDF (24 MW/6 MWh BESS is considered with n_{TS} = 5).

	Steady-State (0.2C)	**Transient State (4C Discharge and 0.2C Recovering Charge)**	**Combined Cycle (Steady-State + Transient State)**	**Manufacture Specific 80% DoD Cycle (0.5C)**
Wear cost per MWh	\$347/MWh	\$981/MWh	\$360/MWh	\$447/MWh
Wear cost per Mode	\$5787/(16.66 MWh/day)	\$3384/ (3.45 MWh/event)	-	\$4291.2/ (9.6 MWh/cycle)
Annual wear cost	\$2,108,867	\$16,922	\$2,125,789	-

The annual cost with an arbitrary number of transient mode (n_{TS}) can be calculated as:

$$Annual\ wear\ cost = E_{TS} \times n_{TS} \times W_{TS} + \left[E_{SS} \times \left(365 - \frac{n_{TS} \times T_{TS}}{24}\right) \times W_{SS}\right] \tag{12}$$

where WTS is the wear cost per MWh for the transient state and WSS is the wear cost per MWh for the steady state. The costs are derived by considering the operating SoC, temperature, and C-rate according to the given pattern for each mode, rendering it possible to predict a relatively accurate lifespan. From (12) and the cycle energy for each mode derived in the previous section, the expected BESS's lifespan can be calculated as:

$$\begin{aligned} Expected\ Life\ Span\ of\ BESS\ for\ FR &= \frac{Battery\ Price}{Annual\ wear\ cost} \\ &= \frac{6\ \text{MWh} \times \$4.6\ \text{M/MWh} = \$27.6\ \text{M}}{\left\{\begin{array}{c} 3.45\ \text{MWh} \times n_{TS} \times \$981 + \\ 16.66\ \text{MWh} \times \left(365 - \frac{n_{TS} \times 1\ \text{h}}{24}\right) \times \$347 \end{array}\right\}} \end{aligned} \tag{13}$$

Considering the same condition that the transient state happens five times per year, as in the previous section, the expected lifespan is estimated to be 13 years, which is substantially different from the base case result (5.1 years) obtained using the I/O energy-based lifecycle evaluation.

Figure 9 shows the BESS's lifespan evaluation. The lifespan change of BESS shows a nonlinear decrease as the number of transient states changes. Therefore, the expected lifespan decreases proportionally with the number of transient states. However, even with 500 transient states annually, the lifespan is still more than eight years because the steady-state cycle ratio is overwhelmingly high; therefore, the transient state does not significantly affect the lifespan.

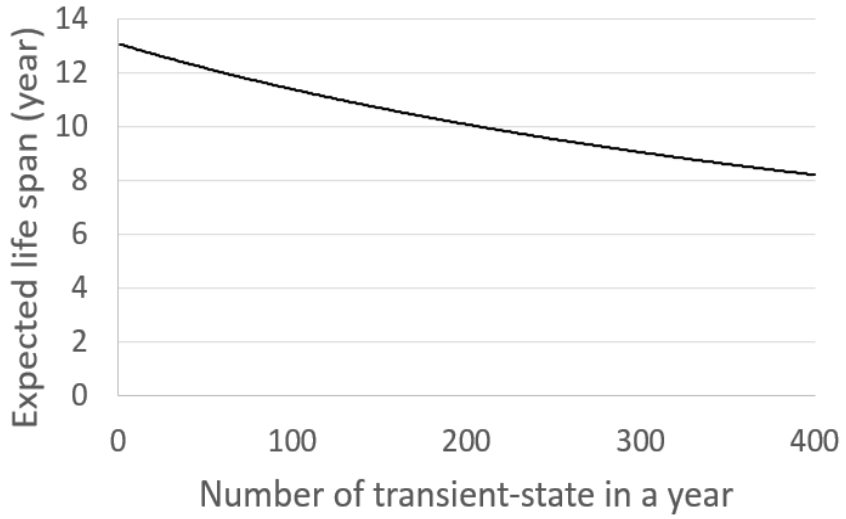


Figure 9. Wear cost for the BESS that costs $4.6 M per a unity 4 C system (4-MW/1-MWh) obtained using the DOD-ACC curve in Figure 4.

4. Impact Analysis on the Operation Parameters

Steady-state operation is the major cause of battery degradation. Subsequently, assessing operation parameters of the steady state is critical from both performance and lifecycle perspectives. Therefore, there is a need to develop a simulator that can evaluate both the performance and corresponding lifecycle expectancy of the BESS by mimicking the actual behaviour of the KEPCO BESS. The description of the simulation model is beyond the scope of this study and has been submitted as a separate article; thus, we present the simulator's basic scheme (Figure 10). As input, actual time-series frequency data is fed into the inverted-grid-equivalent simulator, generating corresponding time-series power variation data for a given power system model. This output is summed to the BESS simulator's output to yield an input to the grid-equivalent model to generate the corresponding frequency variations. This frequency data is fed into the BESS simulator, generating the appropriate charge-discharge operation data. Finally, the battery's lifecycle under a given configuration is evaluated using this operation data and the WDF derived in the previous section.

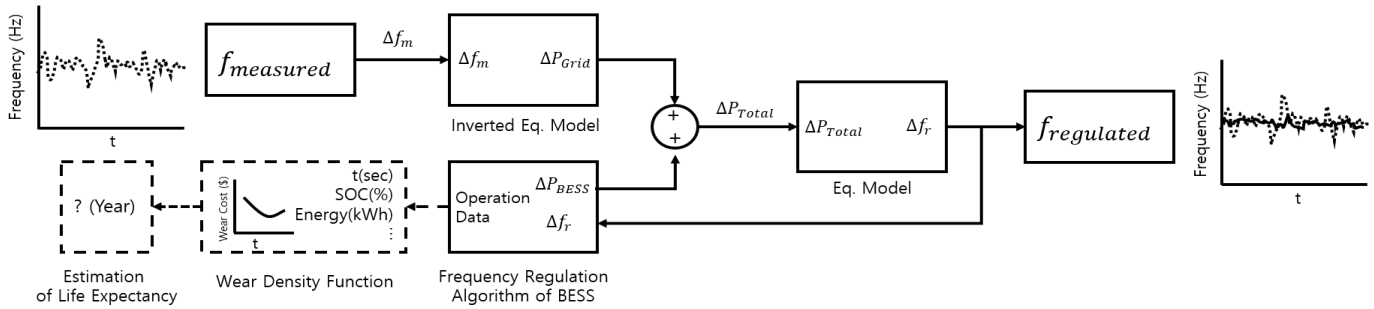


Figure 10. Equivalent model and BESS battery life expectancy model.

The three main parameters governing the BESS driving algorithm for FR, namely, droop, dead-band, and the SoC range, initiate recovery control. Changing any of these parameters affects the operation of the BESS, altering the battery's lifecycle. Further, these parameters' values also change the FR performance. To analyse the performance, we use the frequency's mean absolute deviation (MAD) as a performance measure, which measures the frequency-scattering degree. The smaller the value is, the better the performance achieved; therefore, as the MAD of the frequency becomes smaller, the frequency fluctuation decreases, and a stable FR operation is achieved. The MAD obtained from the actual data

without the BESS is 0.0159 Hz. The performance is evaluated by comparing it with the base case value.

4.1. Droop Rate

Droop is an inversely proportional gain determining the power variation for a given frequency change; to evaluate its impact, simulations are performed for five droop rate levels. The rest of the control parameters (frequency dead-band region and SoC control range) are set to a fixed value from 59.97 to 60.03 Hz and from 63% to 67%, respectively. Figure 11 shows the life expectancy and MAD according to the droop. The applied droop is 0.28%, and the life expectancy is 8.33 years. The lower the droop, the higher the BESS's target output. The higher target output increases the battery's discharge rate, increasing the performance but accelerating degradation and reducing battery life expectancy.

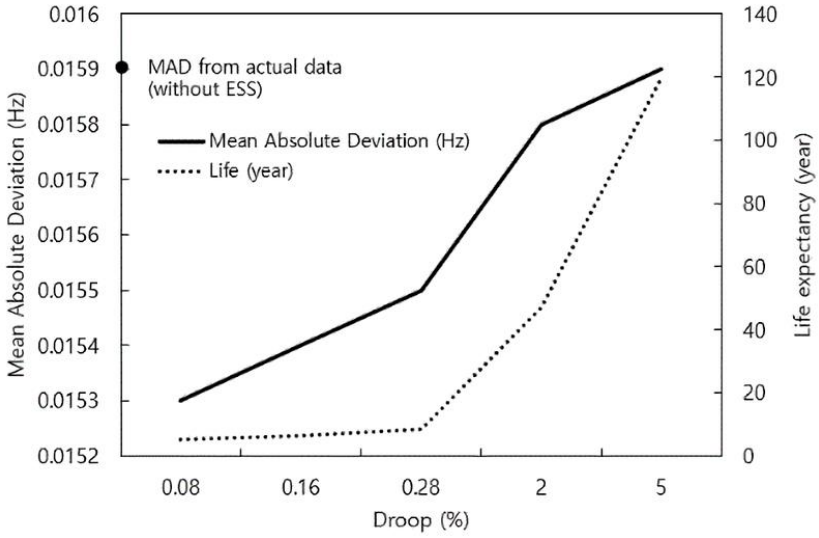


Figure 11. Performance and life evaluation according to droop change.

Conversely, increasing the droop value significantly can dramatically increase the battery life, but the FR performance is similar to when the BESS is not installed. Note that the battery life expectancy over dozens of years does not mean the actual battery can last that long because the battery would deteriorate without a cycle. The result is so because the WDF deploys only lifecycle aspects without considering the storage life, as the lifecycle is a dominant degradation factor for the application.

4.2. Dead-Band

Dead-band is a frequency region where the BESS does not respond to the frequency variation. Currently, the applied value to the system is ±0.03 from 60 Hz. From this value, simulations are performed, decreasing the width of the dead-band for four cases. The droop and SoC recovery ranges are fixed to the current operation value of 0.028% and 63~67%, respectively. Figure 12 shows the resulting lifespan expectancy and frequency MAD. The expected battery lifespan with the currently applied dead-band (±0.03 Hz) is 8.33 years. It can be inferred that a narrow dead-band will cause sensitive operation of the BESS, reducing the battery lifecycle. The simulation result confirms the inference. As the dead-band width decreases, the expected battery life drastically reduces. Specifically, if the dead-band is reduced by 0.01 Hz from the current set value, ±0.03 Hz, the battery's lifespan is halved.

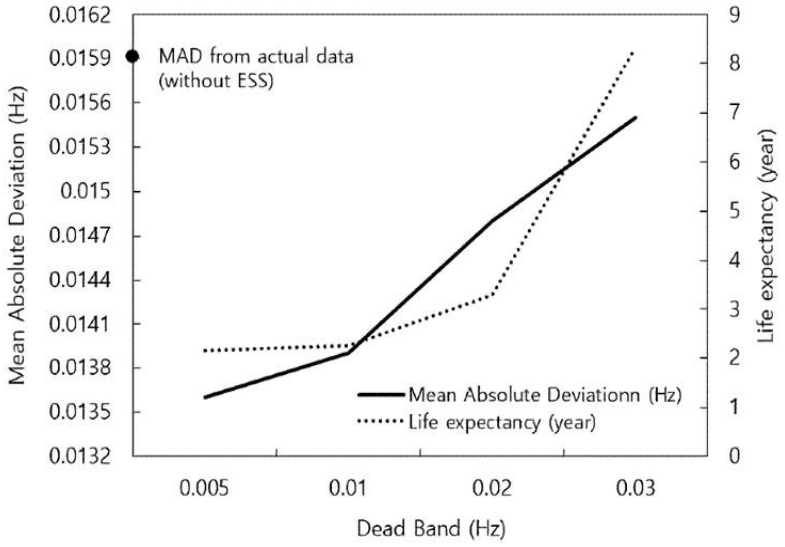


Figure 12. Performance and life evaluation according to dead-band change.

4.3. SoC Recovery Range

During the steady state, the BESS's operation algorithm regulates the SoC to stay within a fixed range, referred to as the SoC recovery range. The lifespan expectancy of the recovery control section was derived from four cases. The currently applied SoC range of the recovery control is ±2% SoC < 63% or SoC > 67% based on 65%. As a control variable, the speed adjustment rate is 0.028% and the frequency dead-band is 59.97 Hz–60.03 Hz.

Figure 13 shows the battery lifespan expectancy and frequency MAD over the recovery control section. When ±2% is selected for the current recovery control, the estimated battery lifespan is 8.33 years. From the frequency MAD, the same performance is obtained when the recovery control condition of the SoC range is 65% ± 2%, ±4%, and ±6%. Therefore, even if the existing SoC range is adjusted more widely, the battery lifespan expectancy can be increased, and the performance can be guaranteed. We have derived the lifespan expectancy and performance by varying the main parameters affecting the BESS's performance and lifespan. Currently, the BESS's operating parameter values for FR have been selected as performance-based parameters based on empirical knowledge. However, the BESS's lifespan must be considered to select the appropriate parameter values, and an economical operation is possible.

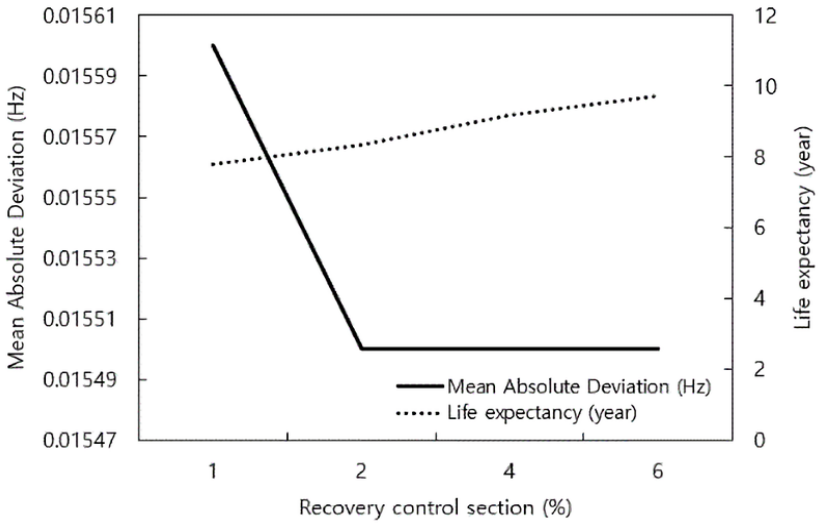


Figure 13. Performance and life evaluation according to SoC recovery range change.

5. Conclusions

Because the battery lifespan expectancy can be calculated differently depending on the BESS's capacity and the operation algorithm, the accurate estimation of the battery's lifespan expectancy is critical in establishing the BESS for FR. The lifespan estimation of the I/O-energy-based method considering actual data was 6.47 years. The battery lifespan expectancy using the WDF was estimated to be ~8.31 years, resulting in a higher lifespan expectancy. Furthermore, an equivalent system model was developed to evaluate the BESS's performance according to the change in operational parameters. Therefore, a tradeoff relationship between the BESS's performance and battery lifespan is deduced. Identifying these parameters in advance of demonstrating this relationship is critical because it can maximise performance and lifespan. Future research will focus on various energy applications of FR using these technical findings.

Author Contributions: Conceptualization, S.H.; methodology, J.P. and H.J.; software, D.K.; validation, J.P. and S.H.; formal analysis, J.P.; investigation, J.P.; resources, J.C. and D.K.; data curation, J.P., J.C. and S.H.; writing—original draft preparation, J.P.; writing—review and editing, J.P. and M.A.A.; visualisation, H.J.; supervision, M.A.A.; project administration, M.A.A. All authors have read and agreed to the published version of the manuscript.

Funding: This work was supported by the Korea Institute of Energy Technology Evaluation and Planning (KETEP) and the Ministry of Trade, Industry & Energy (MOTIE) of the Republic of Korea (No. 20191210301990).

Data Availability Statement: Not applicable.

Conflicts of Interest: The authors declare no conflict of interest.

Nomenclature

μ	Charging and discharging efficiency
ACC	Achievable cycle count
AWC	Average wear cost
BESS	energy storage system
c_t	C-rate
CC	Constant current
C-rate	Rate of charge/discharge
CV	Constant voltage
DOD	depth of discharge
EoL	Specific end-of-life
E_{TS}	Cycle energy during each transient state
Δf	Change in frequency
Δf_m	Change measure frequency
Δf_r	Change regulated frequency
FR	Frequency regulation
I/O	input/output
K	Relationship between generation amount and the frequency variation
KEPCO	Korea Electric Power Corporation
MAD	mean absolute deviation
n_{TS}	Number of annual transient states
ΔP_{BESS}	Change in BESS power
ΔP_{grid}	Change in grid power
ΔP_{total}	Change in total power
Δq	Amount of battery energy during ΔS
q_t	Cycle energy for each time frame
ΔS	SoC interval
S	Instance in the SoC interval
s_t	SoC
SOC	State-of-charge

SoH	State of health
t	Time index during the given period
Δt	Change in time
T_{TS}	Duration of each transient state.
Wd	AWC
WDF	Density function
WSS	Wear cost per MWh for the steady state
WTS	Wear cost per MWh for the transient state

References

1. Khalid, A.; Stevenson, A.; Sarwat, A.I. Overview of Technical Specifications for Grid-Connected Microgrid Battery Energy Storage Systems. *IEEE Access* **2021**, *9*, 163554–163593. [CrossRef]
2. Amoasi Acquah, M.; Kodaira, D.; Han, S. Real-Time Demand Side Management Algorithm Using Stochastic Optimization. *Energies* **2018**, *11*, 1166. [CrossRef]
3. KEPCO to Open Large-Capacity ESS Market for Power Frequency Regulation-ETNews. Available online: http://english.etnews.com/news/article.html?id=20140416200005 (accessed on 12 August 2020).
4. Alt, J.T.; Anderson, M.D.; Jungst, R.G. Assessment of utility side cost savings from battery energy storage. *IEEE Trans. Power Syst.* **1997**, *12*, 1112–1120. [CrossRef]
5. Yun, J.Y.; Yu, G.; Kook, K.S.; Rho, D.H.; Chang, B.H. SOC-based control strategy of battery energy storage system for power system frequency regulation. *Trans. Korean Inst. Electr. Eng.* **2014**, *63*, 622–628. [CrossRef]
6. Serrao, L.; Chehab, Z.; Guezennec, Y.; Rizzoni, G. An aging model of Ni-MH batteries for hybrid electric vehicles. In Proceedings of the 2005 IEEE Vehicle Power and Propulsion Conference, Chicago, IL, USA, 7 September 2005; pp. 78–85.
7. Vetter, J.; Novák, P.; Wagner, M.R.; Veit, C.; Möller, K.C.; Besenhard, J.O.; Winter, M.; Wohlfahrt-Mehrens, M.; Vogler, C.; Hammouche, A. Ageing mechanisms in lithium-ion batteries. *J. Power Sources* **2005**, *147*, 269–281. [CrossRef]
8. Broussely, M.; Biensan, P.; Bonhomme, F.; Blanchard, P.; Herreyre, S.; Nechev, K.; Staniewicz, R.J. Main aging mechanisms in Li ion batteries. *J. Power Sources* **2005**, *146*, 90–96. [CrossRef]
9. Gismero, A.; Schaltz, E.; Stroe, D.I. Recursive state of charge and state of health estimation method for lithium-ion batteries based on coulomb counting and open circuit voltage. *Energies* **2020**, *13*, 1181. [CrossRef]
10. Belt, J.R. *Battery Test Manual for Plug-In Hybrid Electric Vehicles*; Idaho National Lab. (INL): Idaho Falls, ID, USA, 2010.
11. Christophersen, J.P.; Ho, C.D.; Motloch, C.G.; Howell, D.; Hess, H.L. Effects of Reference Performance Testing during Aging Using Commercial Lithium-Ion Cells. *J. Electrochem. Soc.* **2006**, *153*, A1406. [CrossRef]
12. Kim, J.; Chun, H.; Kim, M.; Yu, J.; Kim, K.; Kim, T.; Han, S. Data-Driven State of Health Estimation of Li-Ion Batteries with RPT-Reduced Experimental Data. *IEEE Access* **2019**, *7*, 106987–106997. [CrossRef]
13. Coleman, M.; Lee, C.K.; Hurley, W.G. State of health determination: Two pulse load test for a VRLA battery. In Proceedings of the IEEE Annual Power Electronics Specialists Conference, Jeju, Korea, 18–22 June 2006.
14. Zhang, J.; Zhang, X. A novel internal resistance curve based state of health method to estimate battery capacity fade and resistance rise. In Proceedings of the 2020 IEEE Transportation Electrification Conference & Expo (ITEC), Chicago, IL, USA, 23–26 June 2020; pp. 575–578.
15. Huet, F. A review of impedance measurements for determination of the state-of-charge or state-of-health of secondary batteries. *J. Power Sources* **1998**, *70*, 59–69. [CrossRef]
16. Ng, K.S.; Moo, C.S.; Chen, Y.P.; Hsieh, Y.C. Enhanced coulomb counting method for estimating state-of-charge and state-of-health of lithium-ion batteries. *Appl. Energy* **2009**, *86*, 1506–1511. [CrossRef]
17. Bhangu, B.S.; Bentley, P.; Stone, D.A.; Bingham, C.M. Nonlinear observers for predicting state-of-charge and state-of-health of lead-acid batteries for hybrid-electric vehicles. *IEEE Trans. Veh. Technol.* **2005**, *54*, 783–794. [CrossRef]
18. Lee, S.; Kim, J.; Lee, J.; Cho, B.H. State-of-charge and capacity estimation of lithium-ion battery using a new open-circuit voltage versus state-of-charge. *J. Power Sources* **2008**, *185*, 1367–1373. [CrossRef]
19. Dai, H.; Wei, X.; Sun, Z. A new SOH prediction concept for the power lithium-ion battery used on HEVs. In Proceeding of the 5th IEEE Vehicle Power and Propulsion Conference, Dearborn, MI, USA, 7–10 September 2009; pp. 1649–1653.
20. Kim, I.S. A technique for estimating the state of health of lithium batteries through a dual-sliding-mode observer. *IEEE Trans. Power Electron.* **2010**, *25*, 1013–1022.
21. Plett, G.L. Sigma-point Kalman filtering for battery management systems of LiPB-based HEV battery packs. Part 2: Simultaneous state and parameter estimation. *J. Power Sources* **2006**, *161*, 1369–1384. [CrossRef]
22. Prada, E.; Di Domenico, D.; Creff, Y.; Bernard, J.; Sauvant-Moynot, V.; Huet, F. Simplified Electrochemical and Thermal Model of LiFePO 4 -Graphite Li-Ion Batteries for Fast Charge Applications. *J. Electrochem. Soc.* **2012**, *159*, A1508–A1519. [CrossRef]
23. Han, S.; Han, S.; Aki, H. A practical battery wear model for electric vehicle charging applications. *Appl. Energy* **2014**, *113*, 1100–1108. [CrossRef]
24. Jo, H.; Choi, J.; Agyeman, K.A.; Han, S. Development of frequency control performance evaluation criteria of BESS for ancillary service: A case study of frequency regulation by KEPCO. In Proceeding of the 2017 IEEE Innovative Smart Grid Technologies-Asia, Auckland, New Zealand, 4–7 December 2017; pp. 1–5.

25. Pinsky, N.; O'Neill, L. Southern California Edison Company—Advanced Technology 2131. In *Tehachapi Wind Energy Storage Project Technology Performance Report #3*; Southern California Edison: Rosemead, CA, USA, 2015; pp. 714–934. [CrossRef]
26. Electimes. Available online: http://electimes.com/article.asp?aid=1493265868144076005 (accessed on 12 August 2020).